

# Ladder-Type Polyeazine Based on Intramolecular S···N Interactions: A Theoretical Study of a Small-Bandgap Polymer

Yong-Hui Tian and Miklos Kertesz\*

Department of Chemistry, Georgetown University, 37th & O Street, Washington, D.C. 20057-1227

Received May 18, 2009; Revised Manuscript Received July 7, 2009

**ABSTRACT:** Ladder-type polyeazine (LPEA, **2**), a nitrogen-containing polymer analogous to polyacetylene (PA), is proposed, based on molecule **1** synthesized and characterized earlier.<sup>8</sup> By using density functional theory calculations, we show that the ladder-type structure of the proposed polymer arises from the intramolecular S···N interactions, which reduce the bond length alternation of the polymer and hence lead to a significantly narrower bandgap compared to the parent PA. A  $\sigma$ -conjugated pathway is found along the  $\cdots\text{S}-\text{S}\cdots\text{N}-\text{N}\cdots\text{S}-\text{S}\cdots$  linkage due to the noncovalent S···N interactions and NN through-space interactions. The theoretically predicted electron affinity of the proposed LPEA lies in the range for n-type semiconductors. We examine the energy barrier from the equilibrium geometry to the geometry of uniform bond length pattern and find that the estimated energy barrier is very similar to that of the parent PA.

## 1. Introduction

The search for low-bandgap polymers has been of considerable interest to chemists and physicists. Most of the conducting or semiconducting polymers are composed of  $\pi$ -conjugated systems. In order to achieve low-bandgap polymers (usually smaller than 1.50 eV<sup>1</sup>), a variety of strategies have been proposed, for instance building ladder polymers and incorporating electron donor and acceptor segments in the polymer backbone.<sup>2</sup> For  $\pi$ -conjugated polymers, the bandgap depends on the extent of the band dispersion of the orbitals. Larger  $\pi$ -band dispersion is usually accompanied by higher mobility and smaller bandgaps. Building ladder-type  $\pi$ -conjugated polymers can be an effective way to reinforce the frontier orbital overlap between neighboring unit cells, which reduces the bandgaps. A number of ladder-type semiconducting polymers have been designed such as thienoacene,<sup>3</sup> polyacene,<sup>4</sup> and ladder-type poly(*p*-phenylene) (PPP).<sup>5</sup> Another strategy for gap reduction is based on the idea that the chemical repeat unit should have an odd number of electrons.<sup>6</sup> Systems with an odd number of electrons in the repeat unit (polyacetylene with its CH unit is a prime example) are not metallic because of the tendency for bandgap opening and bond length alternation derived from the concept of Peierls's theorem. The presented system combines the ladder-like topology with an odd number of electrons in the repeat unit of a single system.

Polyacetylene (PA) is one of the "simplest" and most intensely studied archetypical conjugated polymers. Although polyacetylene can achieve metallic conductivity when it is doped with electron donors or acceptors, its intrinsic conductivity lies in the semiconducting range due to a bandgap about 1.5 eV.<sup>7</sup> This bandgap is attributable to the Peierls distortion, the bond length alternation of the carbon–carbon bond distances resulting from the instability of the orbital degeneracy at the Fermi level. In this paper, we introduce a new class of ladder-type polyeazine (LPEA, **2**) derivatives based on S···N interactions as shown in Scheme 1, with the S/N composition of  $n(4\text{S} + 4\text{N}) + 4\text{S} + 2\text{N}$ , where  $n$  is the number of repeat unit. The proposed strategy takes advantage of the X-ray structure of molecule **1** (shown in

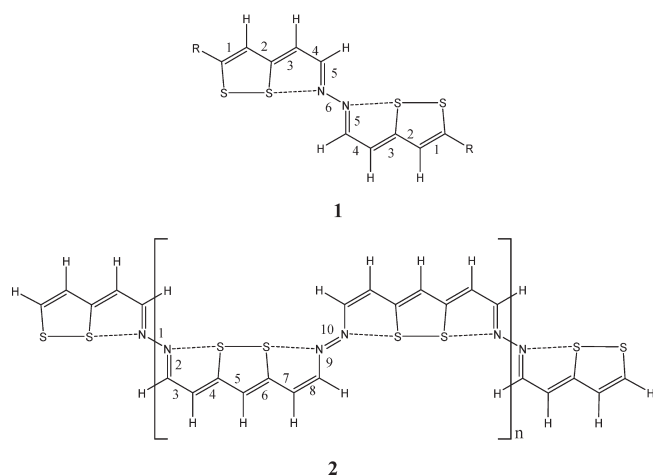
Scheme 1) that was reported over 20 years ago but received little attention.<sup>8</sup> Molecule **1** corresponds to the case of  $n = 0$  in term of the S/N composition. One of the characteristic features of the proposed polymers is the nonbonded S···N interactions that lead to a ladder-type structure along the PA backbone. Herein, we investigated by density functional (DFT) calculations the effect of the S···N interactions on the geometrical and electronic properties of the proposed polymers. Our studies demonstrate that the noncovalent S···N intramolecular interactions effectively planarize the polymer chain and enhance the  $\pi$ -conjugation. Moreover, the  $\cdots\text{S}-\text{S}\cdots\text{N}-\text{N}\cdots\text{S}-\text{S}\cdots$  chain forms a  $\sigma$ -conjugated pathway showing significant band dispersion. The bond length alternation and the band gap of the LPEA are effectively reduced compared to the parent PA.

In a recent study, Houk et al. theoretically explored the potentials of nitrogen-rich oligoacenes as *n*-channel organic semiconductors.<sup>9</sup> The proposed polymers in this paper are also nitrogen-rich, and they have relatively high electron affinity (EA) in combination with low bandgap, which are the characteristic parameters related to the stability and electron transport of *n*-channel polymers.

## 2. Computational Methodology

Previous research shows that, for the chainlike polymers, Becke's half and half hybrid scheme of density functional theory (BHandHLYP)<sup>10</sup> predicts accurate bond length alternations (BLA)<sup>11</sup> while Becke's three-parameter hybrid functional in combination with Lee–Yang–Parr correlation functional (B3LYP)<sup>12</sup> tends to underestimate the BLA. However, the B3LYP bandgaps are more accurate if combined with the BHandHLYP optimized geometry. This trend is shown in Table 1, where the calculated BLA and bandgaps of PA are tabulated. The polymers involved in this study resemble the parent PA in terms of the geometrical and electronic structure. Therefore, the B3LYP//BHandHLYP theory level is expected to perform well for the bandgap prediction for the proposed LPEA. In this study, the proposed oligomers and polymers are geometrically optimized at both B3LYP and BHandHLYP levels, and the bandgaps are calculated at the B3LYP level based on the

\*To whom correspondence should be addressed.

**Scheme 1. Chemical Structures of (1) *N,N*-Bis[2-(5-*tert*-butyl-3*H*-1,2-dithiol-3-ylidene)ethylidene]hydrazine<sup>8</sup> and (2) Ladder-Type Polyene-azine (LPEA)****Table 1. Theoretical BLA and Bandgaps ( $E_g$ ) (in eV) of Polyacetylene**

	BLA <sup>a</sup>	HOMO–LUMO <sup>b</sup>	TDDFT <sup>c</sup>	PBC
B3LYP	0.055 <sup>11b</sup>	1.10 <sup>11b</sup>	1.12	1.21 <sup>11b</sup>
B3LYP//BHandHLYP	0.088 <sup>11b</sup>	1.45	1.27	1.68
expt	0.08–0.09 <sup>13</sup>		1.50 <sup>7</sup>	

<sup>a</sup>BLA is defined as the difference between the long and short CC bonds. <sup>b</sup>The  $E_g$  is calculated by linear extrapolation of the highest occupied molecular orbital (HOMO)–lowest unoccupied molecular orbital (LUMO) gaps of oligomers to infinity. <sup>c</sup>The extrapolated  $E_g$  based on the excitation energy of oligomers.

optimized geometries. On the other hand, although experimental values are unavailable to evaluate the theoretical gaps for the proposed polymers, considering the similarity in structure, the predicted values of LPEA are comparable to that of parent PA as long as the same theory levels are used. Consequently, theoretical computations can predict the trends concerning the effects of the ladder structure on the bandgaps of the proposed LPEA.

Excitation energies for the oligomers are calculated by applying both the time-dependent DFT (TDDFT) and the HOMO–LUMO gaps based on the optimized geometries. The excitation energies and HOMO–LUMO gaps are linearly or quadratically extrapolated as a function of the reciprocal of the total number of  $\pi$  electrons ( $n_\pi$ ) to estimate the polymer bandgaps. The polymer bandgaps are also calculated under periodical boundary condition at the same theory level. The basis set convergence is tested with respect to the bandgap calculations. It is shown that the bandgaps have little change from 6-31G(d) to 6-311G(2d). Addition of a diffuse basis function (6-31+G(d)) changed the bandgap only by about 0.01 eV for the title polymer at the B3LYP//B3LYP level. Therefore, the calculations reported in this study are based on the 6-31G(d) basis set.

The HOMO–LUMO gaps, the bandgaps under periodic boundary conditions (PBC), and the EA calculations are performed employing the Gaussian03 program.<sup>14</sup> The SN bonding energy analysis is carried out with NBO3.<sup>15</sup> The dimerization energies for PA and LPEA are calculated using the Crystal 03 package.<sup>16</sup>

### 3. Results and Discussion

Because of the resemblance in the structure of LPEA to the parent PA, we related the structure and properties of the two polymers and discussed how the structural and electrical properties were changed compared to the parent PA.

**Table 2. Theoretical Bond Lengths (in Å) of 1 and Root Mean Square with Respect to the Experimental Values (Numbering Refers to Scheme 1)**

	$r_1$	$r_2$	$r_3$	$r_4$	$r_5$	$r_6$	rms
B3LYP	1.359	1.435	1.380	1.415	1.308	1.360	0.014
BHandHLYP	1.341	1.439	1.357	1.424	1.284	1.365	0.008
X-ray <sup>a</sup>	1.336	1.429	1.365	1.414	1.293	1.372	

<sup>a</sup>Reference 8.

**Table 3. SN Distances,  $r_{\text{SN}}$  (in Å), and Interaction Energies (in kcal/mol) of the Oligomers of 2 Calculated at B3LYP/6-31G(d)//B3LYP/6-31G(d) Level**

	$r_{\text{SN}}(\text{expt})$	$r_{\text{SN1}}^a$	$r_{\text{SN2}}^a$	$E1(2)$	$E2(2)$
$n = 0$	2.489 <sup>8</sup>		2.515		14.62
$n = 1$	N/A	2.683	2.836	7.67	4.22
$n = 2$	N/A	2.671	2.841	8.02	4.13
$n = 3$	N/A	2.671	2.839	8.02	4.16

<sup>a</sup> $r_{\text{SN1}}$  and  $r_{\text{SN2}}$  refer to the central SN distances.

**Noncovalent  $\text{S} \cdots \text{N}$  Interactions and Quasi-Ladder Structure.** Synthesis of the oligomer 1 has been described, and the structure was characterized by X-ray diffraction.<sup>8</sup> It is shown that the  $\text{S} \cdots \text{N}$  contacts in the molecules are around 2.49 Å, which is significantly shorter than the sum of van der Waals (vdW) radii of sulfur and nitrogen. The molecule is centrosymmetric with a transoid configuration about the N–N single bond. Our calculated bond distances along the polymer backbone are listed in Table 2 in comparison with experimental bond distances. The root-mean-square deviations (rms) are small, and the experimental values agree well with the theoretical predictions. The optimized geometry of the molecule indicates a planar structure with an inversion center.

As shown in Table 3, both B3LYP and BHandHLYP predict SN contacts significantly shorter than the van der Waals distance. Strong noncovalent  $\text{S} \cdots \text{N}$  and  $\text{S} \cdots \text{O}$  bonding is frequently found in crystal structures of organic compounds containing divalent sulfur.<sup>17</sup> The formation of the noncovalent  $\text{S} \cdots \text{N}$  or  $\text{S} \cdots \text{O}$  contacts that produce relatively shorter contacts and therefore stronger interactions than typical vdW interactions are generally ascribed to electron donor–acceptor interactions occurring between the  $\text{sp}^2$  lone pairs of nitrogen or oxygen and the unoccupied  $\sigma^*$  orbitals of the S–X bonds (X is covalently bonded to S).<sup>18</sup> In molecule 1, the short intramolecular SN interactions are expected to be strong according to the considerably short SN distance. To evaluate the SN bonding strength, we calculated the SN interaction energies using the NBO method which is widely used for donor–acceptor interaction analysis. According to this method, the extent of the nonbonded interactions can be approximated with the second-order perturbative stabilization energies,  $E(2)$ , between the donor orbitals and acceptor orbitals.<sup>19</sup> The calculated SN interaction is 14.62 kcal/mol at the B3LYP//B3LYP level. The relatively strong nonbonded SN interactions are consistent with the good NBO orbital overlap between the nitrogen lone pairs and the unoccupied  $\sigma^*$  orbitals corresponding to the S–S bond, as illustrated in Figure 1.

When the oligomer size increases, as exemplified by 3 (Figure 2,  $n = 1$  for 2), each SS bond is in close contact with two nitrogen lone pairs as compared to molecule 1, where each SS bond interacts with only one nitrogen lone pair. As shown in Figure 2, the NBO orbital overlap diagram indicates that at both ends of the central SS bonds the  $\sigma^*$  S–S orbitals are in good overlap with the nitrogen lone pairs. However, one notes that the corresponding SN distances increase compared to those in molecule 1, and correspondingly the interaction

energies are reduced (see Table 3). Moreover, we note that the two SN distances alternate with the longer one corresponding to smaller interaction energy. The weakening of the SN bonding can be explained by the fact that the electron-accepting ability of the  $\sigma^*$  SS bond is reduced after interacting with one nitrogen lone pair, and thus it is less favored to interact with the second nitrogen lone pair. With increasing oligomer size, the SN interactions tend to converge as demonstrated by the trends shown in Table 3.

**Electronic Structure of LPEA.** As discussed previously, B3LYP//BHandHLYP accurately predicts the bandgap for parent PA. Therefore, we used it to calculate the energy gaps. On the other hand, the bandgaps based on B3LYP geometry are also reported in this paper for comparison. The energy gaps are calculated using two complementary approaches. The first approach is based on the DFT HOMO–LUMO energy differences and the TDDFT excitation energies of the oligomers containing up to four repeat units defined by **2** in Scheme 1. The bandgap of the polymer is obtained by both quadratically and linearly extrapolating the HOMO–LUMO gaps or the excitation energies with respect to the reciprocal of the number of  $\pi$ -electron along the backbone.<sup>11b</sup> Parts a and b of Figure 3 show the linear extrapolation plots calculated at the level of B3LYP//B3LYP and B3LYP//BHandHLYP, respectively (see Figure S1 for the quadratic plots). In the second approach, the bandgap is calculated under periodic boundary conditions. The bandgaps obtained with the two approaches are summarized in Table 4. We note that the predicted gaps are about 0.33–0.39 eV smaller than those of the parent PA calculated at the same theory level (refer to Tables 1 and 4). The B3LYP//BHandHLYP predicts gaps 0.2–0.4 eV larger than B3LYP//B3LYP, just as the case for the parent PA. The linearly extrapolated HOMO–LUMO gaps are smaller than

the PBC values, while the quadratic extrapolations are consistent with the PBC calculations. This is because  $E_g$  vs  $1/n_\pi$  deviates slightly from a linear relationship as the polymer chains approach infinite size.<sup>20</sup>

For the parent PA, the calculated BLA is 0.055 and 0.088 Å at B3LYP and BHandHLYP, respectively. For the ladder PA, the estimated BLA is 0.046 and 0.080 Å (only the

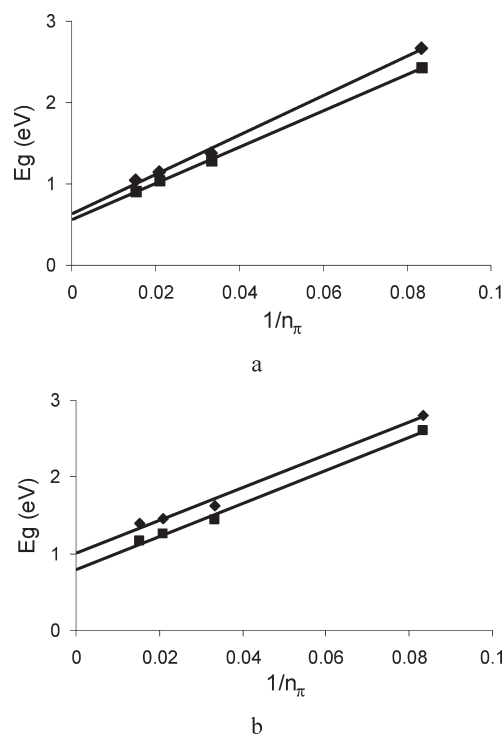


**Figure 3.** DFT HOMO–LUMO gaps (diamonds) and TDDFT excitation energies (squares) as a function of  $1/n_\pi$ : (a) B3LYP//B3LYP level; (b) B3LYP//BHandHLYP.  $n_\pi$  is the number of  $\pi$  electrons on the polymer backbone. Oligomers up to four repeat units were used. (The linear fits are provided to guide the eye.)

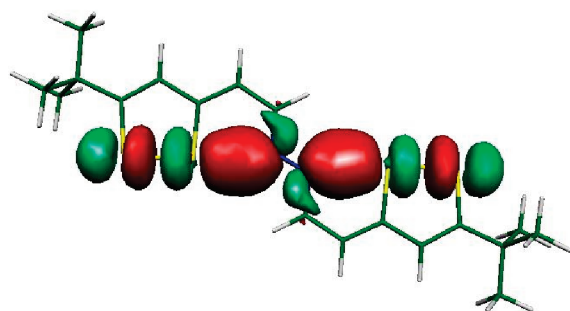


**Figure 1.** NBO orbital overlap diagram of the unoccupied  $\sigma^*$  S–S orbital and the nitrogen n orbital of molecule **1**.

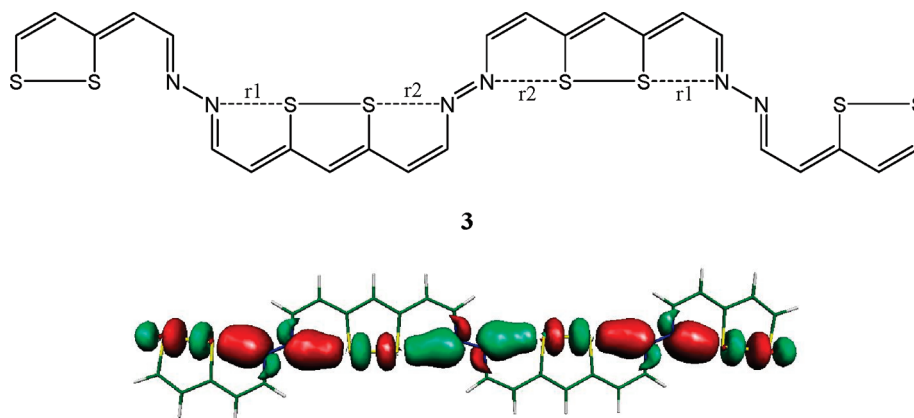


**Figure 2.** Chemical structure of molecule **3** and the NBO orbital overlap diagram of the unoccupied  $\sigma^*$  S–S orbital and the nitrogen n orbital.

**Table 4.** Theoretical BLA<sup>a</sup> (in Å) and Bandgaps ( $E_g$ ) (in eV) of LPEA (**2**)

	BLA	HOMO–LUMO	TDDFT	PBC
B3LYP	0.046	0.64 (0.82)	0.57 (0.60)	0.88
B3LYP//BHandHLYP	0.080	1.01 (1.29)	0.79 (1.00)	1.29

<sup>a</sup> BLA is defined as  $(r_3 - r_4 + r_5 - r_6 + r_7 - r_8)/3$ . Numbering refers to Scheme 1. <sup>b</sup> The values in parentheses correspond to quadratic extrapolation.

Scheme 2. Model Polymer (4) Obtained by Replacing the Dithiol Groups of the Optimized PLA (2) with CH Bonds

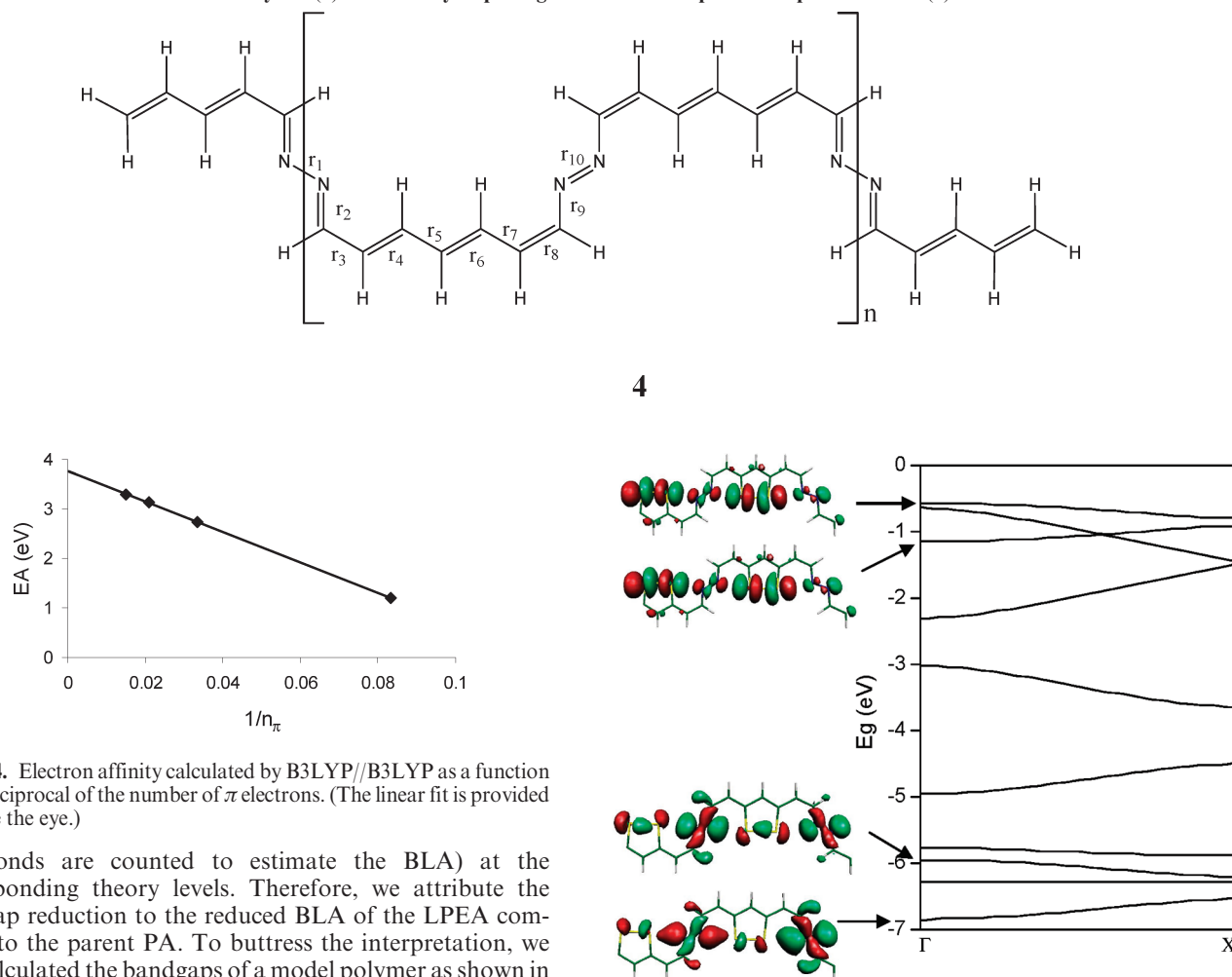


**Figure 4.** Electron affinity calculated by B3LYP//B3LYP as a function of the reciprocal of the number of  $\pi$  electrons. (The linear fit is provided to guide the eye.)

CC bonds are counted to estimate the BLA) at the corresponding theory levels. Therefore, we attribute the bandgap reduction to the reduced BLA of the LPEA compared to the parent PA. To buttress the interpretation, we also calculated the bandgaps of a model polymer as shown in Scheme 2, in which the dithiol groups are replaced by the standard CH bonds, while the other geometrical parameters are kept same as the optimized geometries of the ladder PA. In this model we kept the BLA fixed, and the B3LYP calculated gap of 0.91 eV is almost the same as the gap of the LPEA at the same theory level (0.88 eV).

The EA of the polymer is estimated using the same oligomers as those for the evaluation the bandgaps. The linear plot of the oligomer EA as a function of  $1/n_\pi$  is shown in Figure 4. The estimated value of 3.75 eV is higher than 3.0 eV, which suggests a practical minimum value for n-type semiconductors.<sup>27</sup> At the same time, the calculated EA is below 4.0 eV, which is suggested as an upper limit for the stability of the system against common reducing agents. Therefore, the proposed ladder polymer might be considered as a potential n-type semiconductor. The reason for the relative high EA is the relatively high electronegativity of nitrogen in the polymer backbone.

To elucidate the electronic structure of the ladder polymer, the band structure is presented in Figure 5.

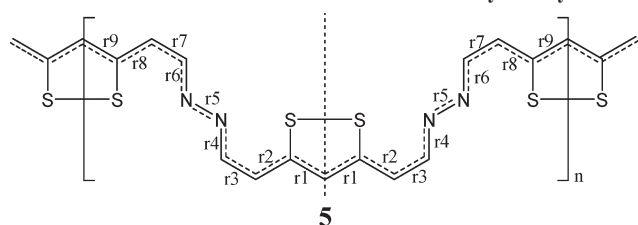
By inspecting the orbitals, we find that the valence band and conduction band correspond to the extension of the  $\pi$  orbitals of the backbone containing carbon and nitrogen, with little participation from the sulfur  $\pi$  lone pairs. The interesting finding is about the bands along the weakly bonded linkages forming a  $\cdots\text{S}-\text{S}\cdots\text{N}-\text{N}\cdots\text{S}-\text{S}\cdots$  chain. We denoted these bands as SN bands. The SN bands are labeled in Figure 5 together with the corresponding crystal orbitals (COs) at the  $\Gamma$  point of the Brillouin zone. As we discussed previously, the n orbitals on nitrogen can interact with  $\sigma^*$  orbitals of the S—S

**Figure 5.** Band structure of the LPEA (2) calculated at the B3LYP//B3LYP level. Five highest occupied and five lowest unoccupied bands are shown. The orbitals corresponding to the SN bands are shown at the  $\Gamma$  ( $k = 0$ ) point. ( $X: k = \pi/a$ ). The Fermi level,  $E_F$ , is near  $-4.0$  eV.

bonds, leading to SN band dispersion. Actually, we find that the occupied SN band (the HOCO-5) indeed has a dispersion of about 0.3 eV. This is small relative to the  $\pi$  band in polyacetylene ( $\sim 5$  eV) but significantly larger than expected from vdW interactions only. As shown by the corresponding orbital, this SN band is composed of  $\sigma^*$  orbitals of the S—S bonds and the n orbitals on nitrogen. The significant dispersion of the SN bands further indicates relative strong SN interactions. One question remains that, since the n orbitals of nitrogen are usually localized, the mixed orbitals of n and  $\sigma^*$  should be localized on the  $\text{N}\cdots\text{S}-\text{S}\cdots\text{N}$  segments, instead of extending along the polymer chain. Actually, the n orbitals on nitrogen interact through-space between the two neighboring nitrogen atoms. Correspondingly, a  $\sigma$ -conjugated pathway opens up along the polymer chain. However, the two bands near  $E_F$  remain  $\pi$  type. Consequently, it appears that the reduction of the bandgap can be interpreted in this system as follows: The ladder topology due to the SN chains provides a reduced bond alternation which in turn leads to a smaller bandgap than in the parent PA.

**Dimerization Energy.** In the ground state, the structure of PA is in a bond length alternation pattern due to a Peierls distortion. The energy barrier between the BLA structures and the hypothetical structure with uniform bond length has been of great interest, since it is related to the formation of



Scheme 3. Structure of LPEA with  $Pm2m$  SymmetryTable 5. B3LYP Calculated Bond Distances<sup>a</sup> and BLA in (Å) of the  $Pm2m$  LPEA (5)

$r_1$	$r_2$	$r_3$	$r_4$	$r_5$	$r_6$	$r_7$	$r_8$	$r_9$
1.397	1.412	1.385	1.340	1.323	1.340	1.386	1.412	1.397

$$\text{BLA} = [(r_2 - r_1) + (r_2 - r_3) + (r_8 - r_7) + (r_8 - r_9)]/6 = 0.011$$

<sup>a</sup>Numbering refers to Scheme 3.

solitons and hence the electrical and magnetic properties of PA and related systems. This energy barrier is called dimerization energy.<sup>22</sup> Our B3LYP calculation shows an energy barrier of 0.32 kcal/mol for each unit cell containing two carbon atoms, which is close to the value by MP2 calculations.<sup>23</sup> Herein, we explore the energy barrier for the LPEA and compare it with that of PA. For both PA and LPEA, as shown in Scheme 3, the higher energy geometry corresponds to the structure with high symmetry of  $Pm2m$  in terms of line group. However, for LPEA, exactly uniform bond length cannot be obtained because of the hetero nitrogen atoms and the unit cell configuration. The optimized geometry parameters with  $Pm2m$  symmetry are listed in Table 5. The bond length alternation of 0.011 Å of the  $Pm2m$  structure is highly reduced compared to 0.055 Å of the optimized equilibrium geometry. The optimized  $Pm2m$  geometry is 2.92 kcal/mol higher in energy than that calculated for the optimized equilibrium geometry. The unit cell of the LPEA is 9 times larger than that of the parent PA in the sense of the number of nitrogen and carbon atoms in the polymer backbone. Therefore, the total energy per unit cell of LPEA divided by nine leads to an energy barrier of 0.33 kcal/mol per two  $\pi$  electrons in the main chain. This barrier happens to be same as that of the parent PA at the same B3LYP level.

#### 4. Conclusions

We proposed a class of ladder-type polyenazine where the ladder is stabilized by intramolecular noncovalent SN interactions. Both the B3LYP//B3LYP and B3LYP//BHandHLYP calculations indicate strong SN interactions in the oligomers according to an NBO analysis. The intramolecular SN interactions account for the planar ladder structure of the proposed polymer. The calculations indicate that the bandgap of the new LPEA is 0.33–0.39 eV smaller than the value of the parent PA (PBC values). We attribute the narrower bandgaps to the reduced BLA of the ladder PA arising from the SN interactions. The calculated EA is high (3.75 eV), and it lies in the range suitable for n-type semiconductors. The band structure analysis shows that the valence band and conduction band are composed of the  $\pi$  orbital of the backbone containing nitrogen and carbon. We found a  $\sigma$ -conjugated pathway along the  $\cdots\text{S}-\text{S}\cdots\text{N}-\text{N}\cdots\text{S}-\text{S}\cdots$  chain, which is formed by the unoccupied  $\sigma^*$  orbital of S–S bonds and the n orbital of nitrogen. The calculations at the same theory level of B3LYP indicate that the dimerization energy of LPEA is nearly same as that of the parent PA. The small barrier indicates that it might be possible to further reduce the gap by further reducing the bond alternation by properly designed repeat units.

**Acknowledgment.** Financial support from the National Science Foundation (Grant DMR-0331710) is gratefully acknowledged. Support by GridChem is acknowledged for computer time.

**Supporting Information Available:** Complete author list of ref 14, optimized geometries and total energies of the polymers reported in the paper, and quadratic extrapolation of the gaps and excitation energies. This material is available free of charge via the Internet at <http://pubs.acs.org>.

#### References and Notes

- (1) Rasmussen, M.; Pomerantz, M. In *Handbook of Conducting Polymers*, 3rd ed.; Skotheim, T. A., Reynolds, J. R., Eds.; CRC: Boca Raton, FL, 2007; Vol. 1, Chapter 12.
- (2) (a) Havinga, E. E.; Hoeve, W.; Wynberg, H. *Synth. Met.* **1993**, 55–57, 299. (b) Kitamura, C.; Tanaka, S.; Yamashita, Y. *Chem. Mater.* **1996**, 8, 570. (c) Ajayaghosh, A. *Chem. Soc. Rev.* **2003**, 32, 181. (d) Salzner, U.; Karalti, O.; Durdagi, S. *J. Mol. Model.* **2006**, 12, 687.
- (3) (a) Zhang, X.; Côté, A. P.; Matzger, A. J. *J. Am. Chem. Soc.* **2005**, 127, 10502. (b) Tian, Y.-H.; Park, G.; Kertesz, M. *Chem. Mater.* **2008**, 20, 3266.
- (4) (a) Coulson, C. A. *Proc. Phys. Soc. A* **1948**, 60, 257. (b) Salem, L.; Longuet-Higgins, H. C. *Proc. R. Soc. London A* **1960**, 255, 435. (c) Kertesz, M.; Lee, Y. S.; Stewart, J. J. P. *Int. J. Quantum Chem.* **1989**, 35, 305. (d) Bendikov, M.; Wudl, F.; Perepichka, D. F. *Chem. Rev.* **2004**, 104, 4891.
- (5) (a) Tian, Y.-H.; Kertesz, M. *Macromolecules* **2009**, 42, 2309. (b) Delnoye, D. A. P.; Sijbesma, R. P.; Vekemans, J. A. J. M.; Meijer, E. W. *J. Am. Chem. Soc.* **1996**, 118, 8717. (c) Zhang, C. Y.; Tour, J. M. *J. Am. Chem. Soc.* **1999**, 121, 8783.
- (6) (a) Jeneke, J. *Nature (London)* **1986**, 322, 345. (b) Kertesz, M.; Lee, Y. S. *J. Phys. Chem.* **1987**, 91, 2690.
- (7) Burroughes, J. H.; Friend, R. H. In *Conjugated Polymers: The Novel Science and Technology of Highly Conducting and Nonlinear Optically Active Materials*; Bredas, J. L., Silbey, R., Eds.; Kluwer Academic: Dordrecht, The Netherlands, 1991; p 555.
- (8) Cuthbertson, A. F.; Glidewell, C.; Liles, D. C. *Acta Crystallogr.* **1982**, B38, 2281.
- (9) Winkler, M.; Houk, K. N. *J. Am. Chem. Soc.* **2007**, 129, 1805.
- (10) Kang, J. K.; Musgrave, C. B. *J. Chem. Phys.* **2001**, 115, 11040.
- (11) (a) Kertesz, M.; Choi, C. H.; Yang, S. *Chem. Rev.* **2005**, 105, 3448. (b) Yang, S.; Kertesz, M. *J. Phys. Chem. A* **2006**, 110, 9771.
- (12) (a) Becke, A. D. *J. Chem. Phys.* **1993**, 98, 5648. (b) Lee, C.; Yang, W.; Parr, R. G. *Phys. Rev. B* **1988**, 37, 785.
- (13) (a) Kahlert, H.; Leitner, O.; Leising, G. *Synth. Met.* **1987**, 17, 467. (b) Yannoni, C. S.; Clarke, T. C. *Phys. Rev. Lett.* **1983**, 51, 1191.
- (14) Frisch, M. J.; et al. et al. *Gaussian 03, Revision E*, Gaussian, Inc., Pittsburgh, PA, **2004**.
- (15) NBO Version 3.1: Glendening, E. D.; Reed, A. E.; Carpenter, J. E.; Weinhold, F.
- (16) Saunders, V. R.; Dovesi, R.; Roetti, C.; Orlando, R.; Zicovich-Wilson, C. M.; Harrison, N. M.; Doll, K.; Civalieri, B.; Bush, I.; D'Arco, Ph.; Llunell, M. *CRYSTAL2003*, University of Torino, Torino, 2003.
- (17) (a) Iwaoka, M.; Takemoto, S.; Okada, M.; Tomoda, S. *Bull. Chem. Soc. Jpn.* **2002**, 75, 1611. (b) Iwaoka, M.; Komatsu, H.; Katsuda, T.; Tomoda, S. *J. Am. Chem. Soc.* **2002**, 124, 1902. (c) Minkin, V. I.; Minyaev, R. M. *Chem. Rev.* **2001**, 101, 1247.
- (18) (a) Iwaoka, M.; Katsuda, T.; Komatsu, H.; Tomoda, S. *J. Org. Chem.* **2005**, 70, 321. (b) Roy, D.; Sunoj, R. B. *J. Phys. Chem. A* **2006**, 110, 5942. (c) Gurm Row, T. N.; Parthasarathy, R. *J. Am. Chem. Soc.* **1981**, 103, 477. (d) Ozen, A. S.; Atilgan, C.; Sonmez, G. *J. Phys. Chem. C* **2007**, 111, 16362. (e) Rosenfield, R. E.; Parthasarathy, R.; Dunitz, J. D. *J. Am. Chem. Soc.* **1977**, 99, 4860.
- (19) Weinhold, F.; Landis, C. R. *Valency and Bonding: A Natural Bond Orbital Donor-Acceptor Perspective*; Cambridge University Press: New York, 2005; p 16.
- (20) Zade, S. S.; Bendikov, M. *Org. Lett.* **2006**, 8, 5234.
- (21) Newman, C. R.; Frisbie, C. D.; da Silva, Filho, D. A.; Bredas, J.-L.; Ewbank, P. C.; Mann, K. R. *Chem. Mater.* **2004**, 16, 4436.
- (22) Springborg, M.; Calais, J.-L.; Goscinski, O.; Eriksson, L. A. *Phys. Rev. B* **1991**, 44, 12713.
- (23) Guo, H.; Paldus, J. *Int. J. Quantum Chem.* **1997**, 63, 345.